LETTERS

Oligomerization of STIM1 couples ER calcium depletion to CRAC channel activation

Riina M. Luik[1]*, Bin Wang[1]*†, Murali Prakriya[1]*†, Minnie M. Wu[1] & Richard S. Lewis[1]

Ca^{2+}-release-activated Ca^{2+} (CRAC) channels generate sustained Ca^{2+} signals that are essential for a range of cell functions, including antigen-stimulated T lymphocyte activation and proliferation[1,2]. Recent studies[3] have revealed that the depletion of Ca^{2+} from the endoplasmic reticulum (ER) triggers the oligomerization of stromal interaction molecule 1 (STIM1), the ER Ca^{2+} sensor, and its redistribution to ER–plasma membrane (ER–PM) junctions[4–8] where the CRAC channel subunit ORAI1 accumulates in the plasma membrane and CRAC channels open[9–12]. However, how the loss of ER Ca^{2+} sets into motion these coordinated molecular rearrangements remains unclear. Here we define the relationships among $[Ca^{2+}]_{ER}$, STIM1 redistribution and CRAC channel activation and identify STIM1 oligomerization as the critical $[Ca^{2+}]_{ER}$-dependent event that drives store-operated Ca^{2+} entry. In human Jurkat leukaemic T cells expressing an ER-targeted Ca^{2+} indicator, CRAC channel activation and STIM1 redistribution follow the same function of $[Ca^{2+}]_{ER}$, reaching half-maximum at ~200 μM with a Hill coefficient of ~4. Because STIM1 binds only a single Ca^{2+} ion[5], the high apparent cooperativity suggests that STIM1 must first oligomerize to enable its accumulation at ER–PM junctions. To assess directly the causal role of STIM1 oligomerization in store-operated Ca^{2+} entry, we replaced the luminal Ca^{2+}-sensing domain of STIM1 with the 12-kDa FK506- and rapamycin-binding protein (FKBP12, also known as FKBP1A) or the FKBP-rapamycin binding (FRB) domain of the mammalian target of rapamycin (mTOR, also known as FRAP1). A rapamycin analogue oligomerizes the fusion proteins and causes them to accumulate at ER–PM junctions and activate CRAC channels without depleting Ca^{2+} from the ER. Thus, STIM1 oligomerization is the critical transduction event through which Ca^{2+} store depletion controls store-operated Ca^{2+} entry, acting as a switch that triggers the self-organization and activation of STIM1–ORAI1 clusters at ER–PM junctions.

The defining feature of store-operated channels is their activation in response to ER Ca^{2+} ($[Ca^{2+}]_{ER}$) depletion. However, their sensitivity to $[Ca^{2+}]_{ER}$ and the factors that determine this sensitivity have never been established, largely because of the technical difficulty of quantifying $[Ca^{2+}]_{ER}$. To address this issue, we generated a Jurkat T cell line stably expressing the Ca^{2+}-sensitive cameleon protein, YC4.2er (see Methods). YC4.2er is selectively retained in the ER, as shown by its colocalization with the resident ER protein calnexin but not with mitochondrial or Golgi markers and by its functional response to agents that deplete ER Ca^{2+} (Fig. 1a and Supplementary Fig. 1). *In situ* calibration of the YC4.2er fluorescence resonance energy transfer signal indicates a responsivity to $[Ca^{2+}]_{ER}$ in the range of ~1 μM to >1 mM (Supplementary Fig. 2).

To determine the dependence of CRAC channel activation on $[Ca^{2+}]_{ER}$, we measured CRAC current (I_{CRAC}) in perforated-patch

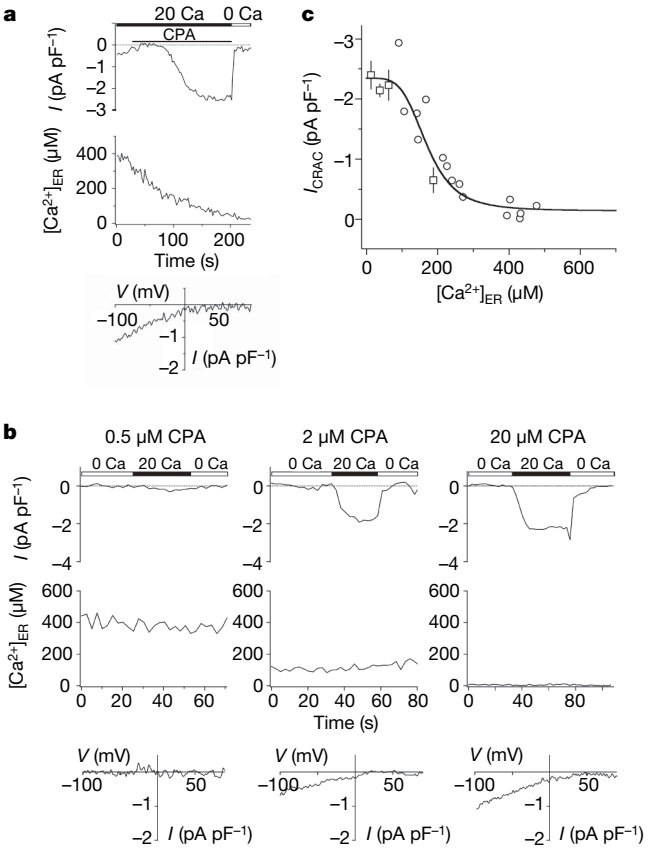

Figure 1 | The dependence of CRAC channel activation on $[Ca^{2+}]_{ER}$. Simultaneous measurements of $[Ca^{2+}]_{ER}$ and I_{CRAC} in individual Jurkat T cells. **a**, Treatment with 20 μM CPA induces an increase in I_{CRAC} (top) that follows a decrease in $[Ca^{2+}]_{ER}$ (middle) monitored with YC4.2er. The current–voltage (*I–V*) relationship shows the inward rectification typical of I_{CRAC} (bottom). In this cell, a small inward current through outwardly rectifying Cl^- channels is also present initially but disappears before I_{CRAC} is induced. Extracellular $[Ca^{2+}]$ in mM is indicated above the bars in **a** and **b**. **b**, Recordings of I_{CRAC} (top) and $[Ca^{2+}]_{ER}$ (middle) under steady-state conditions. Each cell was treated with the indicated CPA concentration for 8–15 min before recording, and CPA was maintained throughout the experiment. *I–V* relationships are typical for I_{CRAC} (bottom). **c**, Steady-state I_{CRAC} and $[Ca^{2+}]_{ER}$ are plotted for 40 cells after treatment with 0.5–20 μM CPA. A fit of the Hill equation with a $K_{1/2}$ of 169 μM and a Hill coefficient of 4.2 is superimposed on the data. Squares, mean ± s.e.m. of 3–12 cells. Circles, single cells (see Supplementary Information).

[1]Department of Molecular and Cellular Physiology, Stanford University School of Medicine, Stanford, California 94305, USA. †Present addresses: Department of Physiology, University of Texas Health Science Center at San Antonio, San Antonio, Texas 78229, USA (B.W.); Department of Molecular Pharmacology and Biological Chemistry, Feinberg School of Medicine, Northwestern University, Chicago, Illinois 60611, USA (M.P.).
*These authors contributed equally to this work.

recordings from Jurkat YC4.2er cells treated with cyclopiazonic acid (CPA), a reversible SERCA (sarco/endoplasmic reticulum Ca^{2+}-ATPase) inhibitor. CPA evokes a time-dependent decline in $[Ca^{2+}]_{ER}$ in parallel with the activation of I_{CRAC} measured in the same cell (Fig. 1a). However, because I_{CRAC} responds slowly to rapid changes of $[Ca^{2+}]_{ER}$, non-stationary measurements like these will distort estimates of the true $[Ca^{2+}]_{ER}$ dependence of the CRAC channel. For this reason, we determined instead the $[Ca^{2+}]_{ER}$–I_{CRAC} relationship under steady-state conditions by pretreating cells with 0.5–20 μM CPA for 8–15 min in the absence of extracellular Ca^{2+} to generate a range of constant $[Ca^{2+}]_{ER}$ values. This passive depletion approach also minimizes spatial variations of $[Ca^{2+}]_{ER}$, allowing the $[Ca^{2+}]_{ER}$ dependence of store-operated Ca^{2+} entry (SOCE) to be determined from whole-cell YC4.2er measurements. After re-addition of 20 mM Ca^{2+} to the bath, current was monitored during brief hyperpolarizations from the resting potential of +30–50 mV at constant $[Ca^{2+}]_{ER}$ (Fig. 1b). The current was identified as I_{CRAC} on the basis of its inwardly rectifying current–voltage relationship , extremely low current noise, and a delayed response to extracellular Ca^{2+} resulting from Ca^{2+}-dependent potentiation (Fig. 1b)[1,13]. Measurements from 40 cells show that I_{CRAC} is a steep function of $[Ca^{2+}]_{ER}$ with half-maximal activation ($K_{1/2}$) at 169 μM and a Hill coefficient of 4.2 (Fig. 1c). Interestingly, a decline of >100 μM from the resting $[Ca^{2+}]_{ER}$ of ~400 μM is required to initiate CRAC channel opening in these cells, which may help to explain how small amounts of ER Ca^{2+} can be released without activating I_{CRAC} in some cells[1].

We next addressed the source of the CRAC channel's steep dependence on $[Ca^{2+}]_{ER}$. Because STIM1 is known to be the Ca^{2+} sensor for SOCE[6,7] and its redistribution to ER–PM junctions is linked to I_{CRAC} activation[6–8,11], we measured the dependence of STIM1 redistribution on $[Ca^{2+}]_{ER}$. Exposure to 0.5–3 μM CPA for >8 min causes a partial redistribution of Cherry–STIM1 to the cell periphery, which can be seen by wide-field imaging at the cell equator (Fig. 2a). We quantified the redistribution of Cherry–STIM1 as the ratio of the mean peripheral fluorescence to the mean total fluorescence (Fig. 2b); this method gives results that agree quantitatively with total internal reflection fluorescence (TIRF) measurements of STIM1 puncta (Supplementary Fig. 3) while facilitating the separation of the cameleon and Cherry fluorescence signals (see Supplementary Information). Measurements from 41 cells show that STIM1 redistribution is a steep function of $[Ca^{2+}]_{ER}$ that closely resembles that of I_{CRAC} activation, with a $K_{1/2}$ of 187 μM and a Hill coefficient of 3.8 (Fig. 2c). The value of $K_{1/2}$ is close to the binding affinity of the recombinant EF-hand plus the sterile alpha motif (SAM) domain of STIM1 measured *in vitro* (K_d = 200–600 μM; ref. 5), consistent with its role as an ER Ca^{2+} sensor. Importantly, the close correspondence between the STIM1 and I_{CRAC} curves indicates that CRAC channels open in direct proportion to the concentration of STIM1 at ER–PM junctions and that the CRAC channel derives its highly nonlinear dependence on $[Ca^{2+}]_{ER}$ from the ER Ca^{2+} dependence of STIM1 redistribution. A recent study of HeLa cells found a similar dependence of STIM1 redistribution on $[Ca^{2+}]_{ER}$ (ref. 14). In that study, the homologue STIM2 redistributed to ER–PM junctions at higher $[Ca^{2+}]_{ER}$ ($K_{1/2}$ = 406 μM) than did STIM1 ($K_{1/2}$ = 210 μM), and it was proposed that STIM2 functions as a homeostatic ER Ca^{2+} sensor by activating ORAI1. Our findings that I_{CRAC} and STIM1 redistribution follow the same function of $[Ca^{2+}]_{ER}$ implies that in Jurkat cells STIM2 activates at most a minor fraction of endogenous CRAC channels, consistent with its low level of expression in T cells[15].

The shape of the STIM1 redistribution curve has important implications for the mechanism underlying SOCE. The Hill coefficient of ~4 shows that puncta formation is a nonlinear process with respect to $[Ca^{2+}]_{ER}$, without necessarily indicating a cooperative mechanism or that the active form of STIM1 is a tetramer. However, the high Hill coefficient implies that STIM1 puncta at ER–PM junctions do not form by the independent accretion of STIM1 monomers, which contain only a single luminal Ca^{2+}-binding site[5], but suggests instead that only oligomers of STIM1 can accumulate at these sites. There are two ways in which STIM1 is known to oligomerize. In resting cells, STIM1 self-associates with an undetermined stoichiometry by means of its cytosolic coiled-coil domains[16,17]; in addition, removal of Ca^{2+} from the EF-hand of STIM1 drives further oligomerization *in vitro*[5] and *in vivo*[4]. Store-dependent oligomerization of STIM1 occurs within seconds, slightly in advance of puncta formation, and a causal role in SOCE has been hypothesized but never tested[4,5].

To address the possible role of STIM1 oligomerization in SOCE, we adopted an approach based on rapamycin-induced protein heterodimerization[18,19]. We replaced the luminal region of Cherry–STIM1 (containing the EF-hand and SAM domains) with a tandem dimer of FK506-binding protein (FKBP12) or a variant of the FKBP-rapamycin binding domain of mTOR (FRB) to generate STIM1 chimaeras that will heterodimerize when bound to a rapamycin analogue (AP21967, or rapalogue). Given that STIM1 is known to self-associate at rest[16,17], rapalogue would thus be expected to link multimers containing FRB with those containing FKBP to form extended oligomers of STIM1 (Fig. 3a). We assayed oligomer formation in HEK293 cells expressing Cherry–FRB–STIM1 and Cherry–FKBP–STIM1 (abbreviated hereafter as F–STIM1) using blue native polyacrylamide gel electrophoresis (BN–PAGE)[20]. The >2-fold increase in apparent mass after rapalogue treatment confirms its ability to oligomerize F–STIM1, and because crosslinking of monomers would be expected to at most double the mass, indicates that the resting state of FRB–STIM1 and FKBP–STIM1 is at least a dimer (Fig. 3b).

We first examined the effects of rapalogue on the localization of F–STIM1 in Jurkat cells. Rapalogue evoked a redistribution of F–STIM1 to the cell periphery that was complete within several minutes (Fig. 3c). Quantitative analysis shows that rapalogue triggers the

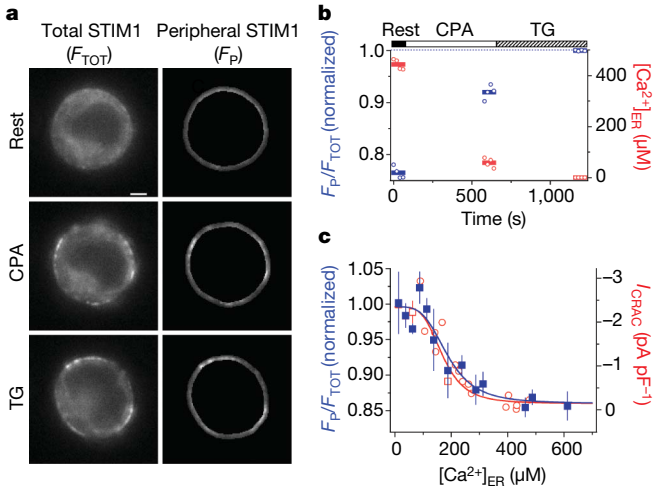

Figure 2 | The $[Ca^{2+}]_{ER}$ dependence of STIM1 redistribution determines the $[Ca^{2+}]_{ER}$-response relation of the CRAC channel. a, Wide-field epifluorescence images of a cell expressing Cherry–STIM1 at rest (top) and after store depletion with 3 μM CPA (middle) and thapsigargin (TG; bottom). The redistribution of Cherry–STIM1 in single cells was monitored as the ratio of the mean fluorescence in the most peripheral 0.5 μm of the cell (F_P, right) to the mean fluorescence of the entire cell (F_{TOT}, left). Scale bar, 2 μm. **b**, In the same cell, STIM1 redistribution is represented by F_P/F_{TOT} normalized to the maximum ratio with TG (blue). F_P/F_{TOT} increases as $[Ca]_{ER}$ (red) declines. Individual data points (open symbols) and the mean responses (bars) are shown. **c**, STIM1 redistribution (F_P/F_{TOT}, blue) is plotted against $[Ca^{2+}]_{ER}$ after treatment with 0–3 μM CPA (means ± s.e.m. of 3–4 cells; 41 cells total). A fit of the Hill equation (blue line) indicates a $K_{1/2}$ of 187 μM and a Hill coefficient of 3.8. Steady-state I_{CRAC} data fitted with the Hill equation are re-plotted from Fig. 1 (red).

redistribution of F–STIM1 as effectively as Ca^{2+}-store depletion induces the redistribution of wild-type STIM1 (Fig. 3d). When examined by TIRF microscopy, the rapalogue-driven peripheral accumulations of F–STIM1 (Fig. 3e) resemble the puncta of wild-type STIM1 that form in response to store depletion (Fig. 3f). Similar results were obtained in HEK293 cells. Rapalogue did not affect the localization of wild-type STIM1 (Fig. 3g), nor did it deplete Ca^{2+} stores (see below). Finally, rapalogue-induced F–STIM1 puncta co-localize with store-depletion-induced green fluorescent protein (GFP)–STIM1 puncta in the same cell, confirming that rapalogue causes F–STIM1 to accumulate at the same ER–PM junctions where STIM1 and ORAI1 are known to interact. Thus, we conclude that oligomerization of STIM1 is sufficient to drive the redistribution of STIM1 to ER–PM junctions.

Heterodimerization of FRB–STIM1 and FKBP–STIM1 also activates endogenous CRAC channels. Rapalogue increased the mean resting $[Ca^{2+}]_i$ in Jurkat cells expressing F–STIM1 (Cherry-positive cells) from 170 ± 11 nM (untreated; $n = 61$) to 388 ± 45 nM (Fig. 4a; $n = 45$), but did not affect $[Ca^{2+}]_i$ in untransfected Jurkat cells. The increased basal $[Ca^{2+}]_i$ was dependent on extracellular Ca^{2+} (Fig. 4a) and was inhibited by 2-aminoethyldiphenyl borate (2-APB) and low concentrations of La^{3+} (Supplementary Fig. 4), consistent with constitutive Ca^{2+} entry through open CRAC channels[1,13]. Importantly, thapsigargin (TG) released similar amounts of ER Ca^{2+} in rapalogue-pretreated and resting cells, indicating that rapalogue stimulates Ca^{2+} entry without depleting Ca^{2+} stores (Fig. 4a). Whole-cell recordings with a high-$[Ca^{2+}]$ pipette solution designed to minimize store depletion confirmed that heterodimerization of FRB–STIM1 and FKBP–STIM1 directly activates I_{CRAC}. In untreated Jurkat cells expressing F–STIM1, I_{CRAC} was negligible on breaking in to the whole-cell recording configuration and developed slowly to a small amplitude, presumably in response to partial store depletion. In contrast, in rapamycin-pretreated cells with visible puncta, large inward currents were evident immediately on breaking in (Fig. 4b) and displayed essential features of I_{CRAC}, including a dependence on extracellular Ca^{2+}, an inwardly rectifying current–voltage relationship (Fig. 4c), low current noise, rapid Ca^{2+}-dependent inactivation, and inhibition by 2-APB and La^{3+} (Supplementary Fig. 4)[13]. The mean current amplitude (2.6 ± 0.6 pA pF^{-1}, $n = 9$) was similar to that produced by Ca^{2+} store depletion in Jurkat cells overexpressing Cherry–STIM1 (ref. 11), consistent with the comparable degrees of STIM1 and F–STIM1 redistribution in response to thapsigargin or rapalogue, respectively (Fig. 3). Together, these results indicate that F–STIM1 oligomers at ER–PM junctions are fully active and provide direct evidence that the oligomerization of STIM1, independently of changes in $[Ca^{2+}]_{ER}$, is sufficient to evoke CRAC channel activation.

We have shown that STIM1 redistribution and I_{CRAC} share a steep dependence on $[Ca^{2+}]_{ER}$, and that oligomerization of F–STIM1 is sufficient to drive puncta formation and CRAC channel activation. These results define the input–output relationship of the CRAC channel and identify STIM1 oligomerization as the primary transduction event through which this relationship is determined. The EF hand and SAM domains of STIM1 seem to serve primarily to control the extent of oligomerization, considering that removal of Ca^{2+} causes a recombinant EF-SAM peptide to oligomerize *in vitro*[5], and that the FRB and FKBP modules in F–STIM1 can effectively substitute for the EF-hand and SAM domains and activate I_{CRAC} when crosslinked by rapalogue. The fact that the latter occurs without Ca^{2+} store depletion suggests that once STIM1 oligomerizes, all subsequent steps leading to SOCE occur independently of ER Ca^{2+}. Thus, we propose that the oligomerization of STIM1 acts as a switch to trigger the self-organization of STIM1 and ORAI1 complexes at ER–PM junctions and the consequent activation of CRAC channels.

How might this oligomerization 'switch' operate? In its resting state Ca^{2+}-bound STIM1 moves freely throughout the ER membrane[4], but after store depletion STIM1 oligomers accumulate in ER subregions located 10–25 nm from the PM, close enough to allow trapping by binding to targets in the PM[8]. These targets have not yet been positively identified, but suggested candidates include ORAI1 (refs 21, 22) or an associated protein[23], as well as PM phospholipids[4,24]. Once localized at ER–PM junctions, STIM1 then promotes

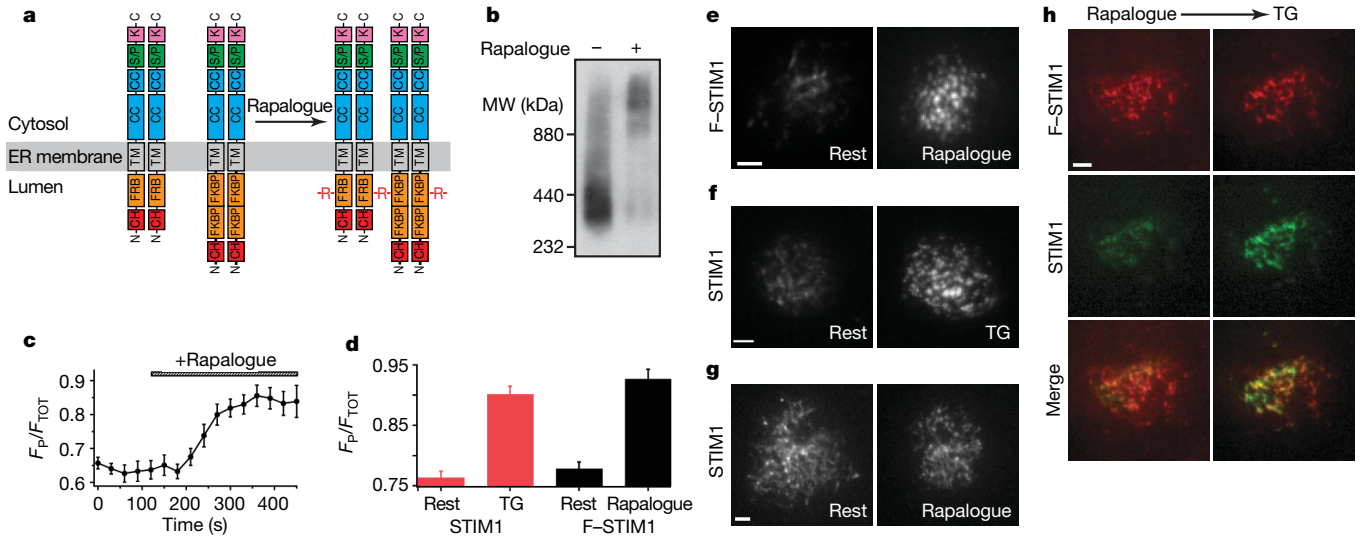

Figure 3 | STIM1 oligomerization induces the accumulation of STIM1 at ER–PM junctions. **a**, The cartoon depicts the oligomerization of F–STIM1 induced by rapalogue (R). At rest, FKBP–STIM1 and FRB–STIM1 are expected to form homo- and hetero-dimers; only intermolecular crosslinks between homodimers are shown here. Abbreviations: CC (coiled-coil), CH (monomeric Cherry), EF (EF hand), K (lysine-rich), SAM (sterile-α motif), S/P (serine–proline-rich). **b**, BN–PAGE and western blot of transiently expressed F–STIM1 harvested from HEK293 cells. Untreated (left) and rapalogue-treated (right) F–STIM1 was detected using a monoclonal anti-STIM1 antibody. MW, molecular weight. **c**, Rapalogue induces a time-dependent peripheral redistribution of F–STIM1 ($n = 10$ cells). **d**, Peripheral redistribution of Cherry–STIM1 by TG (red bars; $n = 31$ for each) and redistribution of F–STIM1 by rapalogue (black bars; $n = 39$, rest; $n = 42$, rapalogue). Values are expressed as mean ± s.e.m. in **c** and **d**. **e**–**h**, TIRF images of Jurkat cells; scale bars, 2 μm. **e**, F–STIM1 before (left) and after (right) incubation with rapalogue. **f**, Cherry–STIM1 before (left) and after (right) store depletion with TG. **g**, Cherry–STIM1 before (left) and after (right) incubation with rapalogue. **h**, F–STIM1 (top row), GFP–STIM1 (middle row) and merged images (bottom row) from a single cell after rapalogue treatment (left column) and subsequent store depletion with TG (right column). Cherry and GFP intensities are scaled to the maximal intensity of each fluorophore after TG treatment.

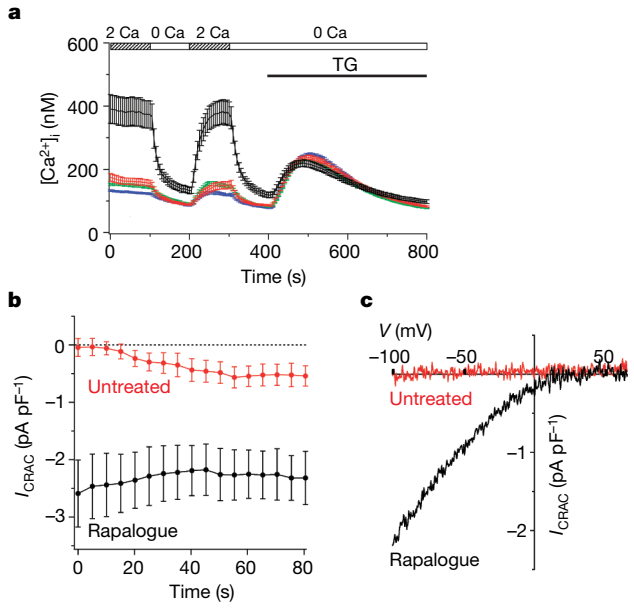

Figure 4 | STIM1 oligomerization activates Ca^{2+} entry through CRAC channels. a, In rapalogue-treated cells expressing F–STIM1 (black, $n = 45$), resting $[Ca^{2+}]_i$ is increased and sensitive to the removal of extracellular Ca^{2+}, indicating constitutive Ca^{2+} entry. In contrast, resting Ca^{2+} influx was largely absent in untreated F–STIM1-expressing cells (red, $n = 61$) and in wild-type Jurkat cells with (green, $n = 617$) or without (blue, $n = 517$) rapalogue. TG-induced Ca^{2+} release in rapalogue-treated cells was similar to that in untreated cells. **b**, I_{CRAC} development during whole-cell recording from rapalogue-treated (black, $n = 9$) and untreated (red, $n = 9$) cells expressing F–STIM1. I_{CRAC} was measured beginning within 5 s of break-in. **c**, *I–V* relations on break-in, showing the inward rectification typical of I_{CRAC} in the rapalogue-treated cell (black) and the absence of current in the untreated cell (red). Values are expressed as mean ± s.e.m. (**a**, **b**).

the accumulation of ORAI1 at apposed sites, leading to channel activation[11,12,25]. Oligomerization may promote the binding of STIM1 to its targets in two ways: an affinity-based mechanism in which a conformational change exposes a previously masked cytosolic binding domain, and an avidity-based mechanism in which clustering of the binding domains increases their local concentration at ER–PM junctions. Both of these mechanisms are likely to contribute to the assembly and function of CRAC channel complexes that constitute the final stage of the store-operated Ca^{2+} entry process.

METHODS SUMMARY

$[Ca^{2+}]_{ER}$ measurements. $[Ca]_{ER}$ was measured in a Jurkat E6-1 cell line stably expressing a modified YC4er (V68L and Q69M; refs 26–28). Cells were pre-treated with CPA (0.5–20 μM) in Ca^{2+}-free Ringer's solution for 8–15 min, and emission intensities at 485 nm and 535 nm were averaged across the cell to yield a raw emission ratio. Ratios were calibrated *in situ* for every cell as described (Supplementary Information).

Heterodimerizer experiments. To generate F–STIM1, mutant FRB and tandem FKBP sequences were substituted for the EF-SAM domain (wild-type STIM1, amino acids 35–207) in Cherry–STIM1 using plasmids provided by Ariad Pharmaceuticals. F–STIM1 was crosslinked using 1 μM rapalogue (AP21967, Ariad Pharmaceuticals). Unless indicated otherwise, cells were pre-incubated in full medium at 37 °C for 30 min, with or without rapalogue, and subsequent measurements were performed at 22–25 °C in standard Ringer's solutions. Time-lapse imaging was performed at 37 °C in full medium with or without rapalogue. Only cells with ~3–10% of the fluorescence of the brightest cells in each experiment were analysed. BN–PAGE was performed essentially as described[20]. A monoclonal antibody against the STIM1 carboxy terminus (1:250; Abnova) and an alkaline-phosphatase-conjugated secondary antibody (1:30,000; Sigma) were used for western blotting.

Perforated-patch and whole-cell recording. I_{CRAC} in YC4.2er cells (Fig. 1) was recorded in the perforated-patch configuration[29] with 20 mM extracellular Ca^{2+}, using a stimulus of a 50-ms step to −100 mV followed by a ramp from −100 to +100 mV, delivered from a holding potential of +30 or +50 mV. Whole-cell recording of I_{CRAC} (ref. 30; Fig. 4) was performed with 20 mM Ca^{2+} Ringer's solution, with stimuli consisting of a 100-ms step to −112 mV followed by a 100-ms voltage ramp from −112 to +88 mV applied from the holding potential of +38 mV beginning within 5 s of break-in.

Full Methods and any associated references are available in the online version of the paper at www.nature.com/nature.

Received 21 January; accepted 8 May 2008.
Published online 2 July 2008.

1. Parekh, A. B. & Putney, J. W. Jr. Store-operated calcium channels. *Physiol. Rev.* **85,** 757–810 (2005).
2. Feske, S. Calcium signalling in lymphocyte activation and disease. *Nature Rev. Immunol.* **7,** 690–702 (2007).
3. Wu, M. M., Luik, R. M. & Lewis, R. S. Some assembly required: constructing the elementary units of store-operated Ca^{2+} entry. *Cell Calcium* **42,** 163–172 (2007).
4. Liou, J., Fivaz, M., Inoue, T. & Meyer, T. Live-cell imaging reveals sequential oligomerization and local plasma membrane targeting of stromal interaction molecule 1 after Ca^{2+} store depletion. *Proc. Natl Acad. Sci. USA* **104,** 9301–9306 (2007).
5. Stathopulos, P. B., Li, G. Y., Plevin, M. J., Ames, J. B. & Ikura, M. Stored Ca^{2+} depletion-induced oligomerization of STIM1 via the EF–SAM region: an initiation mechanism for capacitive Ca^{2+} entry. *J. Biol. Chem.* **281,** 35855–35862 (2006).
6. Zhang, S. L. *et al.* STIM1 is a Ca^{2+} sensor that activates CRAC channels and migrates from the Ca^{2+} store to the plasma membrane. *Nature* **437,** 902–905 (2005).
7. Liou, J. *et al.* STIM is a Ca^{2+} sensor essential for Ca^{2+}-store-depletion-triggered Ca^{2+} influx. *Curr. Biol.* **15,** 1235–1241 (2005).
8. Wu, M. M., Buchanan, J., Luik, R. M. & Lewis, R. S. Ca^{2+} store depletion causes STIM1 to accumulate in ER regions closely associated with the plasma membrane. *J. Cell Biol.* **174,** 803–813 (2006).
9. Prakriya, M. *et al.* Orai1 is an essential pore subunit of the CRAC channel. *Nature* **443,** 230–233 (2006).
10. Vig, M. *et al.* CRACM1 multimers form the ion-selective pore of the CRAC channel. *Curr. Biol.* **16,** 2073–2079 (2006).
11. Luik, R. M., Wu, M. M., Buchanan, J. & Lewis, R. S. The elementary unit of store-operated Ca^{2+} entry: local activation of CRAC channels by STIM1 at ER–plasma membrane junctions. *J. Cell Biol.* **174,** 815–825 (2006).
12. Xu, P. *et al.* Aggregation of STIM1 underneath the plasma membrane induces clustering of Orai1. *Biochem. Biophys. Res. Commun.* **350,** 969–976 (2006).
13. Prakriya, M. & Lewis, R. S. CRAC channels: activation, permeation, and the search for a molecular identity. *Cell Calcium* **33,** 311–321 (2003).
14. Brandman, O., Liou, J., Park, W. S. & Meyer, T. STIM2 is a feedback regulator that stabilizes basal cytosolic and endoplasmic reticulum Ca^{2+} levels. *Cell* **131,** 1327–1339 (2007).
15. Oh-Hora, M. *et al.* Dual functions for the endoplasmic reticulum calcium sensors STIM1 and STIM2 in T cell activation and tolerance. *Nature Immunol.* **9,** 432–443 (2008).
16. Baba, Y. *et al.* Coupling of STIM1 to store-operated Ca^{2+} entry through its constitutive and inducible movement in the endoplasmic reticulum. *Proc. Natl Acad. Sci. USA* **103,** 16704–16709 (2006).
17. Williams, R. T. *et al.* Stromal interaction molecule 1 (STIM1), a transmembrane protein with growth suppressor activity, contains an extracellular SAM domain modified by *N*-linked glycosylation. *Biochim. Biophys. Acta* **1596,** 131–137 (2002).
18. Bayle, J. H. *et al.* Rapamycin analogs with differential binding specificity permit orthogonal control of protein activity. *Chem. Biol.* **13,** 99–107 (2006).
19. Varnai, P., Thyagarajan, B., Rohacs, T. & Balla, T. Rapidly inducible changes in phosphatidylinositol 4,5-bisphosphate levels influence multiple regulatory functions of the lipid in intact living cells. *J. Cell Biol.* **175,** 377–382 (2006).
20. Schägger, H. & von Jagow, G. Blue native electrophoresis for isolation of membrane protein complexes in enzymatically active form. *Anal. Biochem.* **199,** 223–231 (1991).
21. Muik, M. *et al.* Dynamic coupling of the putative coiled-coil domain of ORAI1 with STIM1 mediates ORAI1 channel activation. *J. Biol. Chem.* **283,** 8014–8022 (2008).
22. Yeromin, A. V. *et al.* Molecular identification of the CRAC channel by altered ion selectivity in a mutant of Orai. *Nature* **443,** 226–229 (2006).
23. Varnai, P., Toth, B., Toth, D. J., Hunyady, L. & Balla, T. Visualization and manipulation of plasma membrane–endoplasmic reticulum contact sites indicates the presence of additional molecular components within the STIM1–Orai1 complex. *J. Biol. Chem.* **282,** 29678–29690 (2007).
24. Huang, G. N. *et al.* STIM1 carboxyl-terminus activates native SOC, I_{crac} and TRPC1 channels. *Nature Cell Biol.* **8,** 1003–1010 (2006).
25. Li, Z. *et al.* Mapping the interacting domains of STIM1 and Orai1 in Ca^{2+} release-activated Ca^{2+} channel activation. *J. Biol. Chem.* **282,** 29448–29456 (2007).
26. Miyawaki, A., Griesbeck, O., Heim, R. & Tsien, R. Y. Dynamic and quantitative Ca^{2+} measurements using improved cameleons. *Proc. Natl Acad. Sci. USA* **96,** 2135–2140 (1999).

27. Miyawaki, A. *et al.* Fluorescent indicators for Ca^{2+} based on green fluorescent proteins and calmodulin. *Nature* **388,** 882–887 (1997).
28. Griesbeck, O., Baird, G. S., Campbell, R. E., Zacharias, D. A. & Tsien, R. Y. Reducing the environmental sensitivity of yellow fluorescent protein. Mechanism and applications. *J. Biol. Chem.* **276,** 29188–29194 (2001).
29. Bautista, D. M., Hoth, M. & Lewis, R. S. Enhancement of calcium signalling dynamics and stability by delayed modulation of the plasma-membrane calcium–ATPase in human T cells. *J. Physiol. (Lond.)* **541,** 877–894 (2002).
30. Zweifach, A. & Lewis, R. S. Slow calcium-dependent inactivation of depletion-activated calcium current. Store-dependent and -independent mechanisms. *J. Biol. Chem.* **270,** 14445–14451 (1995).

Supplementary Information is linked to the online version of the paper at www.nature.com/nature.

Acknowledgements We thank N. Bhakta and D. Bautista for assistance and advice during the initial phase of these studies, R. Tsien for the gift of cameleon YC4er, P. Bacchawat for advice on BN–PAGE, and R. Dolmetsch for comments on the manuscript. This work was supported by a grant from the National Institutes of Health (NIH) and the Mathers Charitable Foundation.

Author Information Reprints and permissions information is available at www.nature.com/reprints. Correspondence and requests for materials should be addressed to R.S.L. (rslewis@stanford.edu).

METHODS

Cells, solutions and reagents. Jurkat E6-1 human leukaemic T cells (American Type Culture Collection) and Jurkat YC4.2er cell lines were maintained as described previously[31]. Unless indicated otherwise, experiments were performed at 22–25 °C after cells were attached to poly-D-lysine-coated coverslip chambers and were bathed in Ringer's solution containing (in mM): 155 NaCl, 4.5 KCl, 2 or 20 $CaCl_2$, 1 $MgCl_2$, 10 D-glucose and 5 Na-HEPES (pH 7.4). For Ca^{2+}-free Ringer's solution, $CaCl_2$ was replaced with 1 mM EGTA plus 2 mM $MgCl_2$. To deplete Ca^{2+} stores, cells were exposed to Ca^{2+}-free Ringer's solution supplemented with CPA (0.5–20 μM) or thapsigargin (1 μM). All salts and chemicals were from Sigma unless otherwise stated. Thapsigargin was purchased from LC Laboratories, ionomycin and digitonin were from EMD Biosciences, Inc., monoclonal antibody OKT3 was from eBioscience and Fura-2/AM and Mitotracker Red were purchased from Invitrogen. AP21967 (rapalogue) was provided by Ariad Pharmaceuticals (www.ariad.com/regulationkits).

Plasmids and transfection. Point mutations V68L and Q69M were introduced into the original YC4er (provided by R. Tsien) to generate YC4.2er (refs 26–28). Jurkat E6–1 cells were transfected with YC4.2er by electroporation and selected for stable expression with G418. A monoclonal line with the highest cameleon expression and normal SOCE was used. Construction of Cherry–STIM1 and GFP–myc–ORAI1 were described previously[11].

For the construction of F–STIM1, mutant FRB (pC_4-R_HE) and tandem FKBP (pC_4M-F2E) plasmids were provided by Ariad Pharmaceuticals. The provided variant of FRB binds an analogue of rapamycin (AP21976, or rapalogue) that fails to bind native mTOR, enabling heterodimerization of FRB and FKBP while avoiding potential side effects from inhibition of mTOR kinase activity[18]. FRB- and tandem FKBP-containing STIM1 plasmids were made by engineering two unique restriction sites, a NheI site after Cherry and a MluI site after the SAM domain, into Cherry–STIM1 using site-directed mutagenesis (Quikchange XL, Stratagene). The plasmid was then digested with NheI and MluI to remove the EF-hand and SAM domains (amino acids 35–207 in the wild-type STIM1 sequence). FRB was amplified from pC_4-R_HE using the primers (5′–3′) TGATTAGCTAGCGGTGCTGGTGCTGGTGCTGGTGCTGGTGCTGGTATCCTCTGGCATGAG and (5′–3′) CGACGAATCTCAAAGGGAGCAGGAGCAGGAGCAGGAGCAGGAGCAGGAACGCGTGTAATT to append 11 amino acid linkers (GAGAGAGAGAG) flanked by NheI or MluI restriction sites, respectively. Tandem FKBP (2×FKBP) was amplified from pC_4M-F2E using the primers (5′–3′) TGATTAGCTAGCGGTGCTGGTGCTGGTGCTGGTGCTGGTGCTGGTGCTGGTGGAGTGCAGGTGGAA and (5′–3′) CTGCTGAAGCTGGAGGGAGCAGGAGCAGGAGCAGGAGCAGGAGCAGGAACGCGTGTAATT. Amplified, the FRB and 2×FKBP were separately ligated into NheI- and MluI-digested Cherry–STIM1. The introduction of the NheI site introduced a premature STOP codon, which was removed by site-directed mutagenesis.

FRB–STIM1 and FKBP–STIM1 were transiently transfected into Jurkat E6–1 or Jurkat YC4.2er cells by electroporation as described[8], or into HEK293 cells by lipofection following the manufacturer's protocol (Invitrogen) using 0.5 μg of each construct. Cells were studied 48–72 h after transfection.

Fluorescence microscopy. Wide-field epifluorescence and TIRF microscopy was performed essentially as described using a Zeiss Axiovert 200M microscope[8]. For wide-field epifluorescence microscopy of YC4.2er, cells were excited at 420 nm and dual emission ratios were collected using a 455 DCLP filter cube (Chroma) and by rapidly alternating D485/40 and D535/30 emission filters with a filter changer (Lambda 10-2, Sutter Instruments) positioned at the exit port of the microscope. All images were acquired with a cooled CCD camera (ORCA-ER, Hamamatsu) using 2 × 2 binning (GFP, Cherry, YC4.2er) or 4 × 4 binning (YC4.2er when co-expressed with Cherry).

Fluorescence resonance energy transfer measurements of $[Ca^{2+}]_{ER}$. Background-corrected emission intensities at 535 nm and 485 nm were averaged across the cell to yield a raw F_{535}/F_{485} emission ratio. At the end of every experiment, *in situ* calibration of YC4.2er cells was performed by adding digitonin (50–75 μg ml^{-1}) and ionomycin (10 μM) to permeabilize the plasma membrane while leaving intracellular organelles intact and to equilibrate Ca^{2+} across the ER membrane (Supplementary Fig. 2). In the presence of ionomycin and digitonin, two standard F_{535}/F_{485} ratios (R_1 and R_2) were obtained after exposing the cells to (in mM): 75 K aspartate, 60 KCl, 1 $MgCl_2$, and either 10 EGTA (for R_1) or 20 $CaCl_2$ (for R_2). For every cell, raw F_{535}/F_{485} ratios (R) were normalized using these standard solutions:

$$R_{norm} = (R - R_1)/(R_2 - R_1)$$

where R_{norm} is the normalized YC4.2er ratio[27]. R_{norm} was converted to $[Ca^{2+}]_{ER}$ using a calibration curve determined separately.

A complete calibration curve for YC4.2er (Supplementary Fig. 2) was generated by exposing cells to solutions with various Ca^{2+} concentrations (listed in Supplementary Table 1) after permeabilization with digitonin and ionomycin as described above. The concentrations of K aspartate and KCl were adjusted to maintain constant $[Cl^-]$ and osmolarity. Free $[Ca^{2+}]$ was calculated with MaxChelator software (http://maxchelator.stanford.edu) and subsequently adjusted using a calibrated Ca^{2+}-sensitive electrode (Orion Research Inc.). Normalized F_{535}/F_{485} ratios were calculated as described above and plotted against free $[Ca^{2+}]$, and this relationship was fitted with the following equation using IgorPro (Wavemetrics):

$$[Ca^{2+}]_{ER} = K_d[(R_{norm} - R_{min})/(R_{max} - R_{norm})]^{1/n}$$

where K_d (819 μM) is the apparent dissociation constant, n is 0.54, R_{min} is 0.193 and R_{max} is 1.134. YC4.2er is reported to have an additional, high-affinity binding site for $[Ca^{2+}]_{ER}$ (K_d = 83 nM; ref. 27); the calibration curve was fitted only to the lower affinity site, which reported $[Ca^{2+}]_{ER}$ from ~400 nM to >1 mM (Supplementary Fig. 2b). Thus, in the few cells where R_{norm} fell below the R_{min} for this low-affinity binding site, $[Ca^{2+}]_{ER}$ was assigned a value of 400 nM.

Immunocytochemistry. Jurkat YC4.2er cells were attached to poly-D-lysine-coated glass coverslips and fixed in 4% fresh paraformaldehyde at 22–25 °C for 15 min. For staining with polyclonal anti-calnexin antibody (Stressgen Biotechnologies Corp.), cells were permeabilized for 5 min in cold methanol at –20 °C. For staining with monoclonal anti-golgin-97 (Molecular Probes), cells were permeabilized in 0.5% Triton X-100 in phosphate-buffered saline containing 0.2% bovine serum albumin (PBS/BSA) for 5 min at 22–25 °C. After permeabilization, cells were rinsed three times with PBS and incubated in blocking buffer containing 20 mM glycine, 75 mM NH_4Cl, 0.2% BSA and 1% goat serum in PBS for 1 h. Cells were then incubated with primary antibodies (1:1,000 dilution in blocking buffer) for an additional 1 h and rinsed three times with blocking buffer to remove unbound antibody. Alexa 594-conjugated secondary antibody (Molecular Probes; 1:1,000 dilution in PBS/BSA) was applied for 45 min, followed by three rinses with PBS/BSA. Coverslips were mounted in Vectashield (Vector Laboratories) and viewed with a Zeiss Axiovert 200M microscope (×40 NA1.3 oil), or a Molecular Dynamics Multiprobes 2010 confocal microscope (×40 NA1.3 oil).

Quantification of STIM1 redistribution. A binary mask of the cell periphery was applied to each background-corrected Cherry image by drawing a polygonal region with a width of 0.5 μm around the edge of the cell. The extent of Cherry redistribution was assessed as the mean intensity within the masked region (F_P) divided by the intensity averaged across the whole cell (F_{TOT}). In TIRF experiments, background-corrected Cherry images were thresholded to exclude remaining background fluorescence, and intensity was measured within an outline drawn around the cell footprint in the first frame of each time-lapse series. To compensate for any cell-to-cell differences in the abundance of peripheral ER, changes in redistribution measured by TIRF or wide-field epifluorescence microscopy were normalized to the maximal response obtained in each cell after store depletion with thapsigargin. Mean values of normalized F_P/F_{TOT} or TIRF intensities were calculated from 3–4 images for each data point.

Heterodimerizer experiments. All experiments were performed using 1 μM AP21967. For time-lapse imaging of F–STIM1 redistribution in response to AP21967, cells were imaged using wide-field epifluorescence at 37 °C in full medium. TIRF measurements of F–STIM1 were made at 22–25 °C in 2 mM Ca^{2+} Ringer's solution, before and after treatment with AP21967 for 30 min in full medium at 37 °C on the microscope stage; untreated cells were incubated in full medium alone under the same conditions. Otherwise, cells were pretreated for 30 min in full medium with (treated cells) or without (untreated cells) AP21967 at 37 °C in a CO_2 incubator before imaging at 22–25 °C. Cells overexpressing STIM1 or F–STIM1 at high levels often displayed puncta in the resting state, and correspondingly increased resting $[Ca^{2+}]_i$. This effect of overexpression has also been reported by others for STIM1 (ref. 7). To avoid these effects of overexpression, we restricted analysis to cells with ~3–10% of the fluorescence of the brightest cells in each experiment.

BN–PAGE and western blot analysis. BN–PAGE was performed using the NativePAGE Novex Bis-Tris gel system (Invitrogen) according to the manufacturer's instructions. In brief, 10^7 HEK293 cells expressing F–STIM1 were solubilized using NativePAGE sample buffer supplemented with 1% *n*-dodecyl-β-D-maltoside. For the rapalogue condition, cells were incubated with 1 μM AP21967 for 30 min at 37 °C before solubilization, and 1 μM AP21967 was included in the sample buffer. Coomassie G-250 was added to samples, and 0.5–1% of the sample was loaded onto the NativePAGE Novex 4–16% Bis-Tris gel. Proteins bound to Coomassie G-250 were transferred electrophoretically to Hybond-P membrane (GE Healthcare) in Tris/Glycine buffer (BioRad) for 14 h at 60 mA,

and then fixed with 10% acetic acid and de-stained with methanol. Membranes were blocked with 5% skimmed milk powder in Tris/NaCl buffer (0.05 M Tris, pH 7.4, 0.15 M NaCl, 0.05% Tween 20) and incubated for 8 h at 4 °C with a monoclonal antibody against the STIM1 C terminus (1:250, Abnova). The membrane was washed with Tris/NaCl buffer and then incubated with alkaline phosphatase-conjugated secondary antibody (1:30,000; Sigma) for 1 h at 22–25 °C. After subsequent washing, alkaline phosphatase was detected using Lumi-Phos substrate (Pierce).

Cytosolic $[Ca^{2+}]_i$ measurements. Video microscopic measurements of $[Ca^{2+}]_i$ were performed as described previously[29].

Electrophysiology. Patch-clamp recording was conducted in the standard whole-cell and perforated-patch configurations as previously described[29,30]. The internal solution for whole-cell recording contained (in mM): 140 Cs aspartate, 5 $MgCl_2$, 0.5 $CaCl_2$, 1.2 EGTA and 10 HEPES (pH 7.2 with CsOH). The free $[Ca^{2+}]$ of this solution was calculated to be 146 nM using MaxChelator. For perforated-patch experiments, the internal solution contained (in mM): 115 Cs aspartate, 1 $CaCl_2$, 5 $MgCl_2$, 10 NaCl, 10 HEPES and 100 μg ml^{-1} amphotericin B (pH 7.2 with CsOH). All data were leak-subtracted using currents collected in Ca^{2+}-free Ringer's solution. For whole-cell recording of I_{CRAC} in cells expressing F–STIM1, resting cells were perfused with 20 mM Ca^{2+} Ringer's solution in the cell-attached configuration, and voltage stimuli consisting of a 100-ms step to –112 mV followed by a 100-ms voltage ramp from –112 to +88 mV were applied from the holding potential of +38 mV every 2–5 s, beginning within 5 s of break-in. I_{CRAC} was measured as a 10-ms average at the end of 100-ms pulses to −112 mV, and spontaneous I_{CRAC} was measured from the first voltage step to −112 mV after break-in.

Measuring I_{CRAC} and $[Ca^{2+}]_{ER}$. After 8–15 min pretreatment with CPA (0.5–20 μM) in Ca^{2+}-free Ringer's solution, the perforated-patch configuration was established with YC4.2er Jurkat cells. I_{CRAC} was measured after perfusing the cells with a 20 mM Ca^{2+} Ringer's solution, using a step/ramp stimulus consisting of a 50-ms step to −100 mV followed by a voltage ramp from –100 to +100 mV delivered every 2.5 s from the holding potential of +30 or +50 mV. $[Ca^{2+}]_{ER}$ was measured simultaneously with I_{CRAC} by exciting at 440 ± 10 nm (Chroma) for 40 ms every 2.5 s through a Nikon Fluor ×40 objective (NA 1.3). The emissions from YC4.2er at 485 ± 12.5 nm and 535 ± 12.5 nm were collected simultaneously from an area slightly larger than the cell using two photomultipliers (HC120 05-MOD; Hamamatsu). YC4.2er ratios were calibrated *in situ* as described above.

Image and data analysis. Image analysis was performed using ImageJ software (National Institutes of Health). The dependence of STIM1 redistribution and I_{CRAC} (y) on $[Ca^{2+}]_{ER}$ was described by the Hill equation:

$$y = y_{min} + (y_{max} - y_{min})/(1 + (K_{1/2}/[Ca^{2+}]_{ER})^{n_H})$$

where y_{max} and y_{min} are the maximal and minimal values of STIM1 redistribution or I_{CRAC}, $K_{1/2}$ is the $[Ca^{2+}]_{ER}$ at which these values are half-maximal, and the Hill coefficient, n_H, is a measure of the steepness of the relationship. A curve was fitted by nonlinear least squares in Igor Pro to the entire collection of single-cell data using this equation. For display purposes in Figs 1 and 2, the single-cell responses within 25-μM bins of $[Ca^{2+}]_{ER}$ were averaged and plotted as mean values ± s.e.m. Because of the difficulty of obtaining large numbers of cells in the perforated-patch experiments, some $[Ca^{2+}]_{ER}$ bins contained fewer than three cells; for these bins, I_{CRAC} in single cells is plotted instead (Fig. 1).

31. Prakriya, M. & Lewis, R. S. Potentiation and inhibition of Ca^{2+} release-activated Ca^{2+} channels by 2-aminoethyldiphenyl borate (2-APB) occurs independently of IP_3 receptors. *J. Physiol. (Lond.)* **536**, 3–19 (2001).